C-5A Galaxy Performance & Control

March 19, 2020

Thomas V. Greenhill

ABSTRACT

This report serves to characterize the C-5A Galaxy's dynamic stability characteristics in a qualitative and quantitative manner as a basis for improvement of the aircraft's dynamic stability and control. Through careful analysis of the aircraft's Short Period Mode and Phugoid Mode, the aircraft's Phugoid mode has been determined to be unstable and the aircraft's pitch handling has been determined to be sub-par. Some suggested improvements are proposed, including aerodynamic improvements and implementation of an active feedback control system.

TABLE OF CONTENTS

1. INTRODUCTION:

During initial flight tests at sea level, experimental values of the C-5A's dynamic stability parameters were recorded at an airspeed of 279 ft/s and angle of attack of 11.41 degrees. These values were implemented in the linearized equations of motion in Laplace form to determine the Galaxy's three transfer functions in the longitudinal direction. Based on these transfer functions, the aircraft's uncompensated dynamic stability characteristics were determined and analyzed, and the aircraft's Phugoid mode was found to be unstable. A reduced order analysis was performed to provide a close approximation for the aircraft's Short Period Mode, which was compared to the actual Short Period Mode. The approximation was found to very closely match the actual Short Period Mode, with a relative error in damping ratio and natural frequency of less 1%. Finally, the handling qualities of the C-5A were determined to be sub-par, with heavy pilot workload required to keep the aircraft dynamically longitudinally stable. Several design changes are recommended, including specific changes to the airframe and implementation of an active stabilization controller to damp Phugoid Mode oscillations.

2. RESULTS:

2.1 FLIGHT TEST RESULTS:

First, the flight-tests results were processed and a table of stability parameters was constructed as shown below.

Table 1: C-5A Stability Parameters from Flight Test Data

Parameter (unit)	Value	Parameter (unit)	Value
Airspeed V_∞ (ft/s)	279	Dynamic pressure $\bar{q}$ (lb/ft^2)	N/A
Weight W (lb)	728,000	Wing area S (ft^2)	6,200
Wing span b (ft)	219.17	Wing chord $\bar{c}$ (ft)	30.93
c.g. ($\bar{c}$)	0.25	Trim AOA α_{trim} (deg)	11.41
I_{xx} (slug-ft^2)	3.25*10^7	I_{yy} (slug-ft^2)	3.28*10^7
I_{zz} (slug-ft^2)	6.15*10^7	I_{xz} (slug-ft^2)	-3.34*10^6
X_u (1/s)	-0.0111	X_α (ft/s^2)	-5.58
Z_u (1/s)	-0.107	Z_α (ft/s^2)	-124
Z_{δ_e} (ft/s^2)	-11.5	M_α (1/s^2)	-0.76
$M_{\dot{\alpha}}$ (1/s)	-0.169	M_q (1/s)	-0.67
M_{δ_e} (1/s^2)	-1.049	M_u (1/ft.s)	-0.00007

2.2 TRANSFER FUNCTIONS:

Using the longitudinal linearized equations of motion in the Laplace domain, shown below, the transfer functions for airspeed, $\frac{u(s)}{\delta_e(s)}$, angle of attack, $\frac{\alpha(s)}{\delta_e(s)}$ and pitch angle $\frac{\theta(s)}{\delta_e(s)}$ outputs with elevator deflection input are determined.

$$\begin{bmatrix} (s - X_u - X_{T_U}) & -X_\alpha & g * \cos(\Theta_1) \\ -Z_u & s * (U_1 - Z_{\dot{\alpha}}) - Z_\alpha & -(Z_q + U1) * s + g * \sin(\Theta_1) \\ -(M_u + M_{T_u}) & -(M_{\dot{\alpha}} * s + M_\alpha + M_{T_\alpha}) & (s^2 - M_q * s) \end{bmatrix} \begin{bmatrix} \frac{u(s)}{\delta_e(s)} \\ \frac{\alpha(s)}{\delta_e(s)} \\ \frac{\theta(s)}{\delta_e(s)} \end{bmatrix} = \begin{bmatrix} X_{\delta_e} \\ Z_{\delta_e} \\ M_{\delta_e} \end{bmatrix} \dots \dots (1)$$

Assuming zero initial conditions and with the help of MATLAB (see the Appendix section for sample code), the following transfer functions are computed.

$$\frac{\boldsymbol{u(s)}}{\boldsymbol{\delta_e(s)}} = \frac{\mathbf{0.23}*(\boldsymbol{s}+\mathbf{171.6})*(\boldsymbol{s}+\mathbf{0.3547})}{(\boldsymbol{s^2}-\mathbf{0.0004399}\boldsymbol{s}+\mathbf{0.00789})*(\boldsymbol{s^2}+\mathbf{1.295}\boldsymbol{s}+\mathbf{1.063})} \ldots\ldots(2)$$

$$\frac{\boldsymbol{\alpha(s)}}{\boldsymbol{\delta_e(s)}} = \frac{-\mathbf{0.041219}*(\boldsymbol{s}+\mathbf{26.12})*(\boldsymbol{s}\text{\^{}}\mathbf{2}+\mathbf{0.01064}\boldsymbol{s}+\mathbf{0.01195})}{(\boldsymbol{s^2}-\mathbf{0.0004399}\boldsymbol{s}+\mathbf{0.00789})*(\boldsymbol{s^2}+\mathbf{1.295}\boldsymbol{s}+\mathbf{1.063})} \ldots\ldots(3)$$

$$\frac{\boldsymbol{\alpha(s)}}{\boldsymbol{\delta_e(s)}} = \frac{-\mathbf{1.042}*(\boldsymbol{s}+\mathbf{0.4226})*(\boldsymbol{s}+\mathbf{0.005902})}{(\boldsymbol{s^2}-\mathbf{0.0004399}\boldsymbol{s}+\mathbf{0.00789})*(\boldsymbol{s^2}+\mathbf{1.295}\boldsymbol{s}+\mathbf{1.063})} \ldots\ldots(4)$$

3. DISCUSSION:

3.1 MODAL CHARACTERISTICS:

The characteristic equation of all three transfer functions $\frac{u(s)}{\delta_e(s)}$, $\frac{\alpha(s)}{\delta_e(s)}$, $\frac{\theta(s)}{\delta_e(s)}$, is extracted from their common denominator:

$$\boldsymbol{P_1(s)} = (\boldsymbol{s^2} - \mathbf{0.0004399}\boldsymbol{s} + \mathbf{0.00789}) * (\boldsymbol{s^2} + \mathbf{1.295}\boldsymbol{s} + \mathbf{1.063}) \ldots\ldots(5)$$

From this characteristic equation, we can easily identify the Short Period Mode and Phugoid Mode based on the general form of the characteristic equation for an aircraft's longitudinal modes of dynamic motion (immediately below) and knowledge that $\omega_{N_{PH}} < \omega_{N_{SP}}$.

$$(\boldsymbol{s^2} + \mathbf{2} * \boldsymbol{\zeta_{SP}} * \boldsymbol{\omega_{N_{SP}}} * \boldsymbol{s} + \boldsymbol{\omega_{N_{SP}}^2}) * (\boldsymbol{s^2} + \mathbf{2} * \boldsymbol{\zeta_{PH}} * \boldsymbol{\omega_{N_{PH}}} * \boldsymbol{s} + \boldsymbol{\omega_{N_{PH}}^2}) = \mathbf{0} \ldots\ldots(6)$$

The Short Period Mode and Phugoid Modes hence have the following characteristic polynomials (respectively).

$$P_{SP}(s) = s^2 + 1.295s + 1.063 \ldots\ldots (7)$$

$$P_{PH}(s) = s^2 - 0.0004399s + 0.00789 \ldots\ldots (8)$$

In order to characterize the C-5A's dynamic stability, the pole locations of the aircraft's longitudinal transfer functions must be considered by finding the zeros of the characteristic equations. A graphical representation of the pole locations of the above transfer functions is created and shown below.

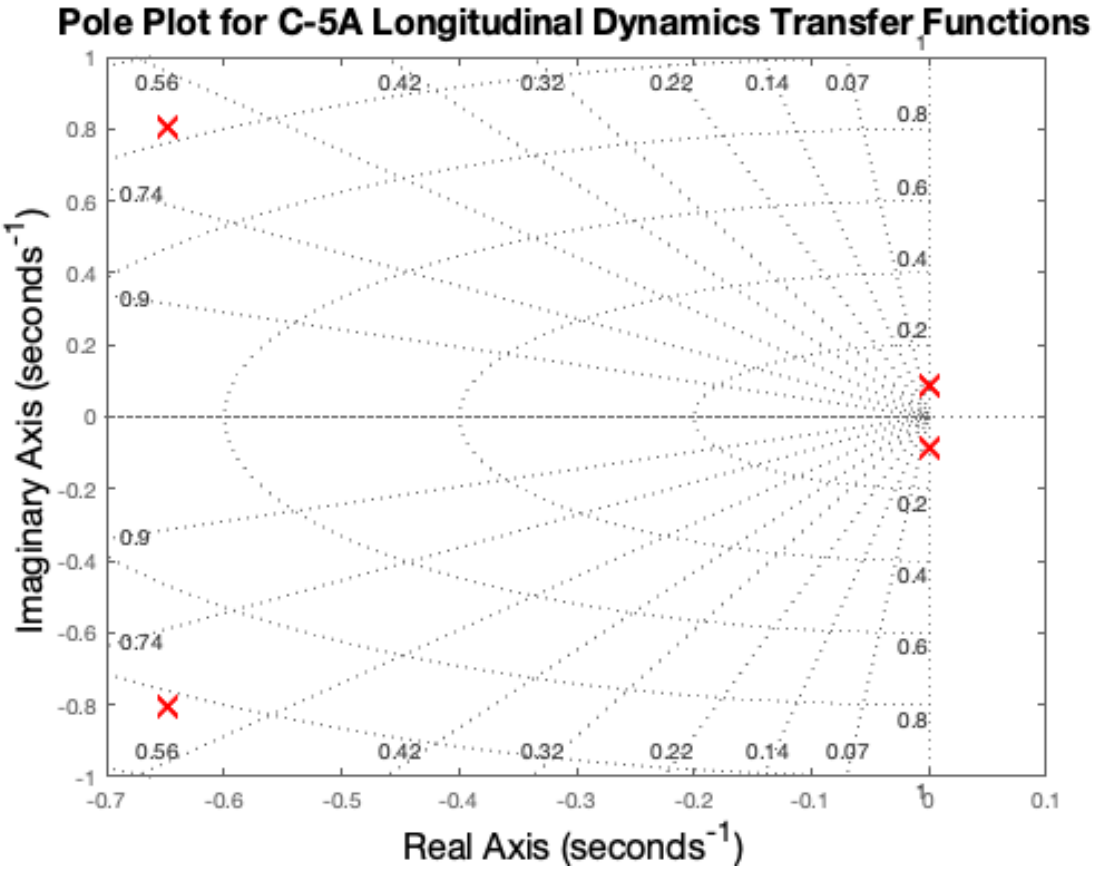

Figure 1: Pole Plot of Longitudinal Dynamics Transfer Functions

The Short Period Mode poles are clearly far left of the imaginary axis, and the Phugoid Mode poles can be seen very near the imaginary axis. This indicates that the Short-Period Mode

is stable and that the Phugoid mode is either marginally stable or unstable. The poles locations of both modes of the form $(\sigma, j\omega)$ are directly calculated and tabulated:

Table 2: Pole Locations of Short Period and Phugoid Modes

Mode	Real Part (σ)	Imaginary Part ($j\omega$)
Short Period	- 0.6475	+ 0.8021
	- 0.6475	- 0.8021
Phugoid	+ 0.0002199	+ 0.08882
	+ 0.0002199	- 0.08882

Table 2 indicates that the Phugoid Mode pole locations are very close to the imaginary axis in the right half plane (RHP) and are hence unstable poles. This indicates that after a very long time, diverging pitch oscillations will occur due to the bounded-input bounded-output (BIBO) unstable Phugoid Mode. The pole locations for the Short Period Mode are in the left half plane (LHP) and have nonzero imaginary parts, indicating that damped oscillation will occur. Hence, the Short Period Mode is BIBO stable. Due to the very long time period required for the oscillations to diverge, the Phugoid Mode behavior can be easily damped by a pilot or simple control system. Overall, though, the C-5A is dynamically longitudinally unstable without the presence of an active controller.

3.2 TIME RESPONSES:

Using MATLAB, time response plots of each transfer function with unit impulse and unit step inputs are created. As discussed in Section 3.1, slowly diverging oscillations occur over the course of several minutes.

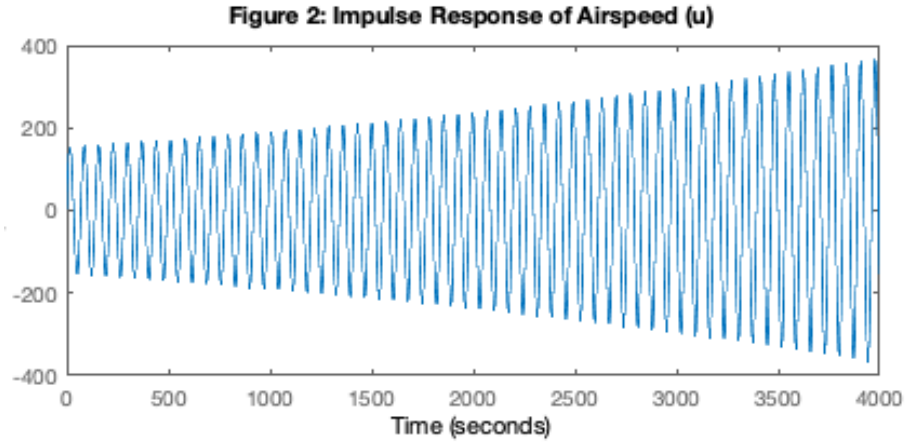

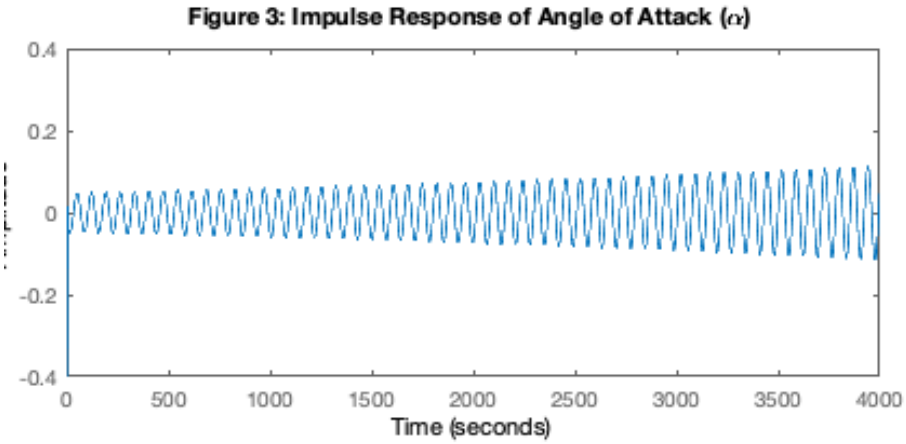

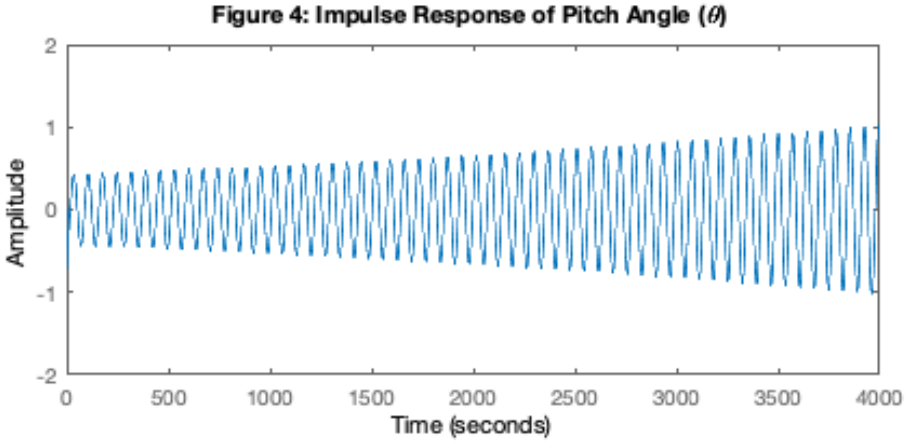

Figures 2-4: Impulse Responses of u, α, θ

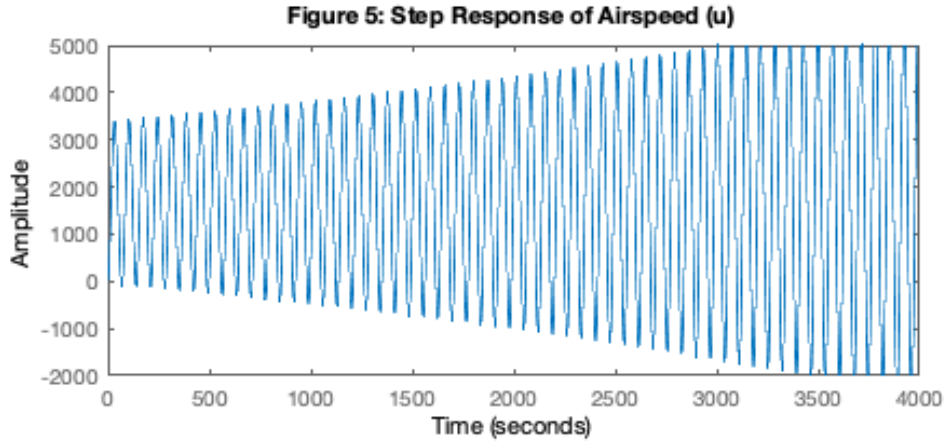

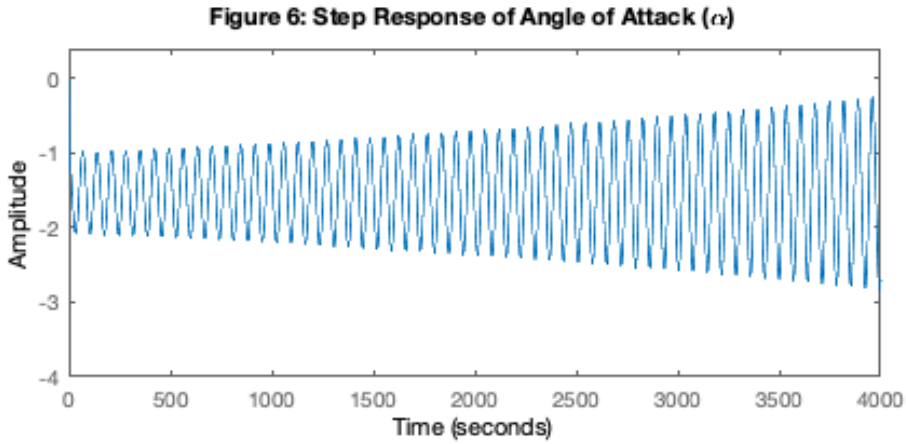

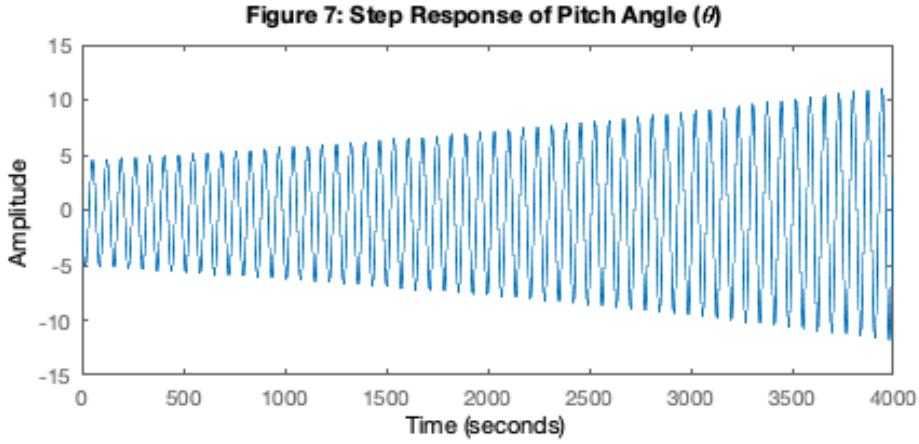

Figures 5-7: Step Responses of u, α, θ

3.3 REDUCED ORDER ANALYSIS:

Now, a reduced order analysis is performed to reduce the characteristic equation in Equation 5 to a Short Period approximation of the general form shown in Equation 9 below.

$$s^2 - \left(M_q + \frac{Z_\alpha}{U_1} + M_{\dot{\alpha}}\right) * s + \left(\frac{Z_\alpha * M_q}{U_1}\right) = 0 \ldots \ldots (9)$$

Implementing values from Table 1, the Short Period Mode approximation is thus described by Equation 10.

$$s^2 + 1.283 * s + 1.058 = 0 \ldots \ldots (10)$$

The natural frequencies (ω_n) and damping ratios (ζ) for both the reduced characteristic equation (Equation 10) and the non-reduced characteristic equation (Equation 5) are tabulated below and compared to evaluate the validity of the reduced order approximation.

Table 3: Damping Ratio and Natural Frequency for Reduced and Non-Reduced Characteristic Equation

	Mode	ζ	ω_n (rad/s)
Non-Reduced	**Phugoid**	- 0.0025	0.0888
	Short Period	0.6281	1.0308
Reduced	**Short Period**	0.6240	1.0285

The reduced order analysis has eliminated the Phugoid Mode and yielded a Short Period Mode with very similar damping ratio and natural frequency as the original. The relative error between the original and the approximation is tabulated and displayed below.

Table 4: Relative Error of Damping Ratio and Natural Frequency

Parameter	Relative Error (%)
ζ	0.65
ω_n	0.22

With a relative error of less than 0.7%, it is safe to say that the reduced order approximation provides a close approximation for the actual Short Period Mode. The impulse response for both the actual Short Period Mode and its reduced order approximation are now plotted.

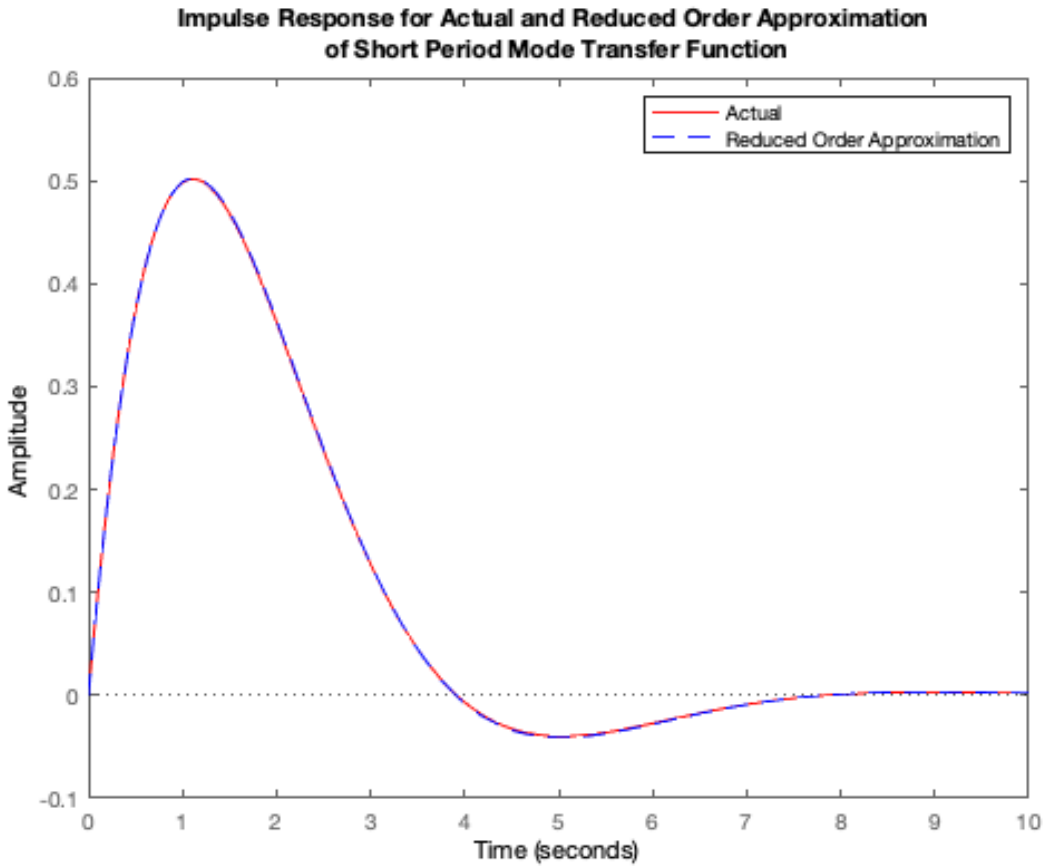

Figure 8: Impulse Response for Actual and Reduced Order Approximation of C-5A Short Period Mode

Upon investigation of Figure 8, it becomes abundantly clear that the reduced order approximation for the C-5A's short period mode is indistinguishable from the aircraft's actual short period mode and is hence a very good approximation. The short period mode is also clearly stable; it quickly damps the oscillation caused by the unit impulse input as we expect.

3.4 HANDLING QUALITIES INVESTIGATION:

The C-5A's handling qualities are now analyzed using the handling quality levels for flight Phase B (flight phase categories are provided in the Appendix) as provided by Tables 5 and 6 below.

Table 5: Short Period Mode Damping Ratio Limits for Category B Flight Phase

	ζ Minimum	**ζ Maximum**
Level 1	0.30	2.00
Level 2	0.20	2.00
Level 3	0.15	No maximum

Table 6: Phugoid Mode Damping Ratio Requirements for Category B Flight Phase

	Requirement
Level 1	$\zeta_{PH} > 0.04$
Level 2	$\zeta_{PH} > 0$
Level 3	$T_2 > 55s$

Recall the values for ζ_{PH} and ζ_{SP} for the non-reduced characteristic polynomial provided in Table 3 above: $\zeta_{PH} = .6281$ and $\zeta_{SP} = -0.0025$. Also, recall the real parts of the roots of the characteristic equation for the Phugoid Mode from Table 2: $Re(p_{PH}) = 0.0002199$. Using this value, we can compute T_2 based on the following relationship.

$$\boldsymbol{T_2 = \frac{0.693}{Re(p)}} \quad \textbf{... ... (11)}$$

The solution to Equation 11 yields $T_2 = 3151.43\ seconds > 55\ seconds$. We can thus conclude that the C-5A falls under Level 1 for its Short Period Mode characteristics and under Level 3 for its Phugoid Mode characteristics. Overall, the C-5A's longitudinal handling characteristics fall under Level 3. Clearly this aircraft is difficult to control and its handling characteristics must be addressed.

3.5 SUGGESTED AERODYNAMIC DESIGN IMPROVEMENTS:

Several aerodynamic improvements can be undertaken to increase Phugoid Mode stability. Although it is detrimental to fuel efficiency and flight performance, increasing total airframe drag will increase Phugoid mode damping by reducing the kinetic energy during the potential energy to kinetic energy exchange. Decreasing the horizontal tail size or distance from C.G. to horizontal tail aerodynamic center would also improve phugoid damping by decreasing the Phugoid natural frequency, $\omega_{n_{PH}}$. Shifting the C.G. further aft would also likely improve Phugoid stability, but if this method is chosen, special care must be taken to ensure positive static margin is conserved. Furthermore, I advise performing some experiments in which the stabilizer's angle of attack relative to the wing is varied slightly; ensuring that the horizontal tail and wing have the same angle of incidence will increase Phugoid Mode stability. Overall, anything that increases Phugoid Mode damping through mechanical or aerodynamic changes will make the aircraft more stable in this mode and in turn improve the aircraft's handling characteristics based on the criteria provided in Table 6.

3.6 SUGGESTED ACTIVE FEEDBACK CONTROL SYSTEM:

If the aerodynamic design changes recommended in Section 3.5 are determined to be unfeasible or too costly, I suggest pursuing a frequency domain approach to classical feedback

control system design to stabilize the aircraft's unstable Phugoid Mode. The steps for designing an appropriate control system are as follows.

Control System Design Procedure:

1. Determine transient requirements. In this case, a choice of peak time, $t_p = 10\ seconds$ and overshoot percent, $\%\ O.S. \leq 2\%$ seem reasonable. Using these values, extract the values for ζ and ω_n.
2. Shape the controller-plant return ratio transfer function to match the transfer function below.

$$\boldsymbol{G_c G_p = \frac{\frac{\omega_n}{2*\zeta}}{s*\left(\frac{s}{2*\zeta*\omega_n}+1\right)}} \boldsymbol{\ldots\ldots (12)}$$

The Bode plot for the generalized return-ratio transfer function above is provided in the figure below. At low frequencies, high gain provides good target following and fast disturbance rejection capabilities. The magnitude plot crosses the 0 dB line at -20 dB/decade, providing the system with good stability and robustness. At high frequencies, the system has very low gain, providing good sensor noise rejection qualities.

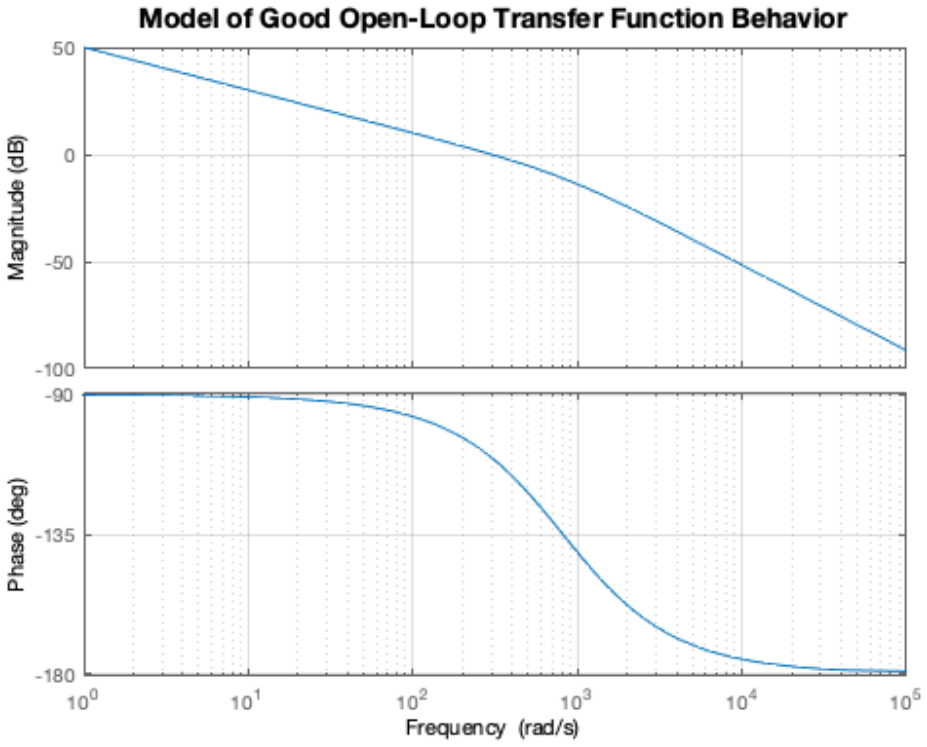

Figure 9: Bode Plot of Good Return Ratio Transfer Function Behavior

3. Recall the Phugoid mode transfer function, G_p, and Extract G_c from Equation 12.

Control System Design Execution:

First, execute step 1 with the relationships for ζ and ω_n as follows.

$$\boldsymbol{\zeta = -\frac{\ln\left(\frac{\%OS}{100}\right)}{\sqrt{\pi^2+\left(\ln\left(\frac{\%OS}{100}\right)\right)^2}} \ldots\ldots (13)}$$

$$\boldsymbol{t_p = \frac{\pi}{\omega_n * \sqrt{1-\zeta^2}} \ldots\ldots (14)}$$

Solving for damping ratio and natural frequency, respectively, yields $\zeta = 0.7797$ and $\omega_n = 0.5017$.

Next, shape the return ratio as outlined in step 2 and find:

$$\boldsymbol{G_c G_p = \frac{0.2517}{s*(s+0.7824)}} \ldots\ldots (15)$$

Recall the Phugoid mode transfer function for one of the longitudinal motion parameters, u, for example $\boldsymbol{G_{p_u} = \frac{0.23*(s+171.6)*(s+0.3547)}{\left(s^2-0.0004399s+0.00789\right)}}$ and perform simple algebra to extract G_c from Equation 15.

$$\boldsymbol{G_c = \frac{0.913776*s*(s+0.3547)*(s+0.782351)}{s^2-0.00044*s+0.00789}} \ldots\ldots (16)$$

This transfer function in the Laplace domain characterizes a controller which fulfills all of the specified requirements. The response to a unit impulse input and a unit step input are plotted below.

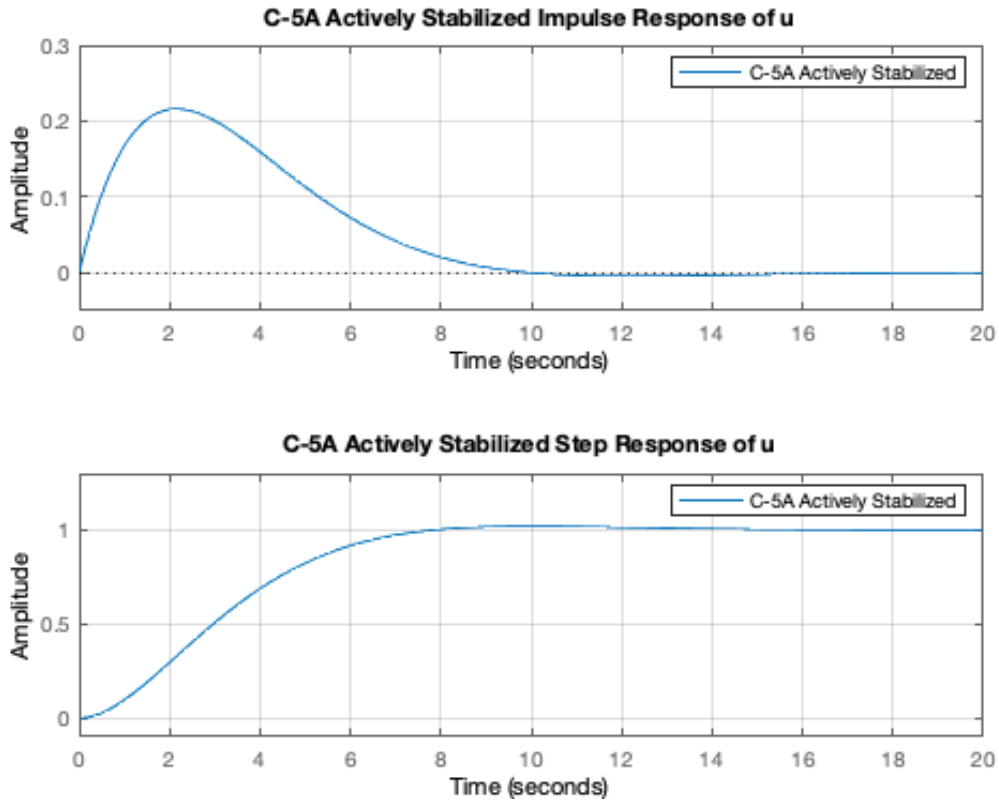

Figure 10: Time Response of C-5A With Active Stabilization System

The airspeed response is only shown here, but because all three dynamic longitudinal stability transfer functions have the same characteristic equation, the stabilization capability of this controller will be well suited for all three of these transfer. The system's performance is analyzed using MATLAB to ensure that the design requirements are met.

```
Performance =

  struct with fields:

       RiseTime: 4.7698
   SettlingTime: 7.1813
    SettlingMin: 0.9077
    SettlingMax: 1.0200
      Overshoot: 1.9987
     Undershoot: 0
           Peak: 1.0200
       PeakTime: 10.0061
```

Figure 11: Controller-Plant Performance for Proposed Controller

Of course, the time-domain parameters can be adjusted and the controller gain changed accordingly, but this example highlights just how easy it is to design a robust active controller to help stabilize the C-5A and reduce pilot workload. When actually implementing a control system such as this one, it is crucial that a sensor speed to loop speed ratio of no less than 5 times is achieved to ensure unity feedback and avoid sensor dynamics.

4. CONCLUSION:

Through analysis of the C-5A's dynamic longitudinal modes from flight test data, it was found that its Short Period Mode is stable and that its Phugoid Mode is unstable. The aircraft's handling qualities were determined to be sub-par and several suggestions were proposed to increase stability and decrease pilot workload.

The design modification procedure should focus on increasing the aircraft's Phugoid Mode damping ratio, ζ_{PH} through aerodynamic design changes or implementation of an active feedback controller. In the event that aerodynamic changes are found to be unfeasible, an example covering the design procedure for an active feedback controller was provided and its functionality was showcased.

5. REFERENCE:

[1] Yechout, T. R. (2014). Introduction to aircraft flight mechanics: performance, static stability, dynamic stability, classical feedback control, and state-space foundations. Reston, VA: American Inst. of Aeronautics and Astronautics.

[2] Kong, Z., EAE 129 Stability and Controls of Aerospace Vehicles. University of California, Davis.

[3] Assadian, F., EME 172 Automation and Controls of Engineering Systems. University of California, Davis.

[4] Sadraey, M. H. (2013). Aircraft design: a systems engineering approach. Chichester: Wiley.

6. APPENDIX:

6.1 FLIGHT OPERATION CATEGORIES

Category	Examples of flight operation
A	1. Air-to-air combat (CO); 2. Ground attack (GA); 3. Weapon delivery/launch (WD); 4. Aerial recovery (AR); 5. Reconnaissance (RC); 6. In-flight refueling (receiver) (RR); 7. Terrain following (RF); 8. Antisubmarine search (AS); 9. Close formation flying (FF); and 10. Low-altitude parachute extraction (LAPES) delivery.
B	1. Climb (CL); 2. Cruise (CR); 3. Loiter (LO); 4. In-flight refueling in which the aircraft acts as a tanker (RT); 5. Descent (D); 6. Emergency descent (ED); 7. Emergency deceleration (DE); and 8. Aerial delivery (AD).
C	1. Takeoff (TO); 2. Catapult takeoff (CT); 3. Powered approach (PA); 4. Wave-off/go-around (WO); and 5. Landing (L).

Table 7: Flight Category Classifications

6.2 MATLAB CODE:

```
%% EAE 129 Final Project
clc
clear all
close all

%% Defining Variables
v_inf = 279;
W = 728000;
b = 219.17;
x_cg = 0.25;
I_xx = 3.25*10^7;
I_zz = 6.15*10^7;
X_u = -0.0111;
Z_u = -0.107;
Z_d_e = -11.5;
M_a_dot = -0.169;
M_d_e = -1.049;
S = 6200;
c_bar = 30.93;
a_trim = 11.41;
I_yy = 3.28*10^7;
I_xz = -3.34*10^6;
X_a = -5.58;
Z_a = -124;
M_a = -0.76;
M_q = -0.67;
M_u = -0.00007;
```

```
theta = 0;
%% Determination of Transfer Functions

s = tf('s')

TF = inv([s-X_u -X_a 32.2; -Z_u s*v_inf-Z_a -v_inf*s; -(M_u) -(M_a_dot*s+M_a)
s^2-M_q*s])*[0;Z_d_e;M_d_e];
TF = minreal(TF);
TFu = zpk(TF(1))
TFa = zpk(TF(2))
TFt = zpk(TF(3))


%% Pole-Zero Plot

pz = pzplot(TF)
grid on
xlabel('Real Axis','FontSize',16)
ylabel('Imaginary Axis','FontSize',16)
title('Pole Plot for C-5A Longitudinal Dynamics Transfer
Functions','FontSize',16)
set(pz.allaxes.Children(1).Children,'MarkerSize',12,'Color','r','LineWidth',2
)

p1 = vpa(pole(TFu),4)

%% Plotting The 3DoF Tiem Responses
close all

t = 0:0.1:4000;

figure('Position',[200 200 500 800])
subplot(3,1,1)
impulse(TF(1,1),t)
title('Figure 2: Impulse Response of Airspeed (u)')
axis([0 4000 -400 400])

subplot(3,1,2)
impulse(TF(2,1),t)
title('Figure 3: Impulse Response of Angle of Attack (\alpha)')
axis([0 4000 -0.4 0.4])

subplot(3,1,3)
impulse(TF(3,1),t)
title('Figure 4: Impulse Response of Pitch Angle (\theta)')
axis([0 4000 -2 2])
% close

figure('Position',[200 200 500 800])
subplot(3,1,1)
step(TF(1,1),t)
title('Figure 5: Step Response of Airspeed (u)')
axis([0 4000 -2000 5000])
```

```
subplot(3,1,2)
step(TF(2,1),t)
title('Figure 6: Step Response of Angle of Attack (\alpha)')
axis([0 4000 -4 0.4])

subplot(3,1,3)
step(TF(3,1),t)
title('Figure 7: Step Response of Pitch Angle (\theta)')
axis auto

%% Reduced Order Analysis
close all

ROA = s^2-(M_q+Z_a/v_inf+M_a_dot)*s+(Z_a*M_q/v_inf-M_a);

p2 = zero(s^2-(M_q+Z_a/v_inf+M_a_dot)*s+(Z_a*M_q/v_inf-M_a))
[wn1,Z1] = damp(TFu);
[wn2,Z2] = damp(1/ROA);

wn1 = wn1(3);
Z1 = Z1(3);
wn2 = wn2(2);
Z2 = Z2(2);
%% Comparing the Response of Actual and Approx Short Period Modes to Unit
Impulse Input
close all
SP_act = wn1^2/(s^2+2*Z1*wn1*s+wn1^2);
SP_aprx = wn2^2/(s^2+2*Z2*wn2*s+wn2^2);

imp = figure
impulse(SP_act,'r');
hold on
impulse(SP_aprx,'b--');
legend('Actual','Reduced Order Approximation')
title(sprintf('Impulse Response for Actual and Reduced Order Approximation
\nof Short Period Mode Transfer Function'))

%% Control system design
close all
RR = 0.2517/(s*(s+0.7824));
GcGp = 0.2517/(s*(s+0.7824))/(1+0.2517/(s*(s+0.7824)))
figure
subplot(2,1,1)
impulse(GcGp)
grid on
legend ('C-5A Actively Stabilized')
axis([0 20 -.05 0.3])
title('C-5A Actively Stabilized Impulse Response of Airspeed (u)')

subplot(2,1,2)
step(GcGp)
grid on
legend ('C-5A Actively Stabilized')
axis([0 20 -.1 1.3])
title('C-5A Actively Stabilized Step Response of Airspeed (u)')
```

```
Performance  = stepinfo(GcGp)
```